Ultrashort Echo-Time Magnetic Resonance Imaging Sequence in the Assessment of Systemic Sclerosis-Interstitial Lung Disease

Nicholas Landini, MD,† Martina Orlandi, MD, PhD,‡*
Mariaelena Occhipinti, MD, PhD,† Cosimo Nardi, MD, PhD,†
Lorenzo Tofani, MStat,‡ Silvia Bellando-Randone, MD, PhD,‡
Pierluigi Ciet, MD, PhD,§‖ Piotr Wielopolski, PhD,‖ Thomas Benkert, PhD,¶
*Cosimo Bruni, MD,‡ Silvia Bertolo, MD,**
Alberto Moggi-Pignone, MD, PhD,# Marco Matucci-Cerinic, MD, PhD,‡
Giovanni Morana, MD, and Stefano Colagrande, MD†*

Purpose: To test respiratory-triggered ultrashort echo-time (UTE) Spiral VIBE-MRI sequence in systemic sclerosis-interstitial lung disease assessment compared with computed tomography (CT).

Material and Methods: Fifty four SSc patients underwent chest CT and UTE (1.5 T). Two radiologists, independently and in consensus, verified ILD presence/absence and performed a semiquantitative analysis (sQA) of ILD, ground-glass opacities (GGO), reticulations and honeycombing (HC) extents on both scans. A CT software quantitative texture analysis (QA) was also performed. For ILD detection, intra-/inter-reader agreements were computed with Cohen K coefficient. UTE sensitivity and specificity were assessed. For extent assessments, intra-/inter-reader agreements and UTE performance against CT were computed by Lin's concordance coefficient (CCC).

Results: Three UTE were discarded for low quality, 51 subjects were included in the study. Of them, 42 QA segmentations were accepted. ILD was diagnosed in 39/51 CT. UTE intra-/inter-reader K in ILD diagnosis were 0.56 and 0.26. UTE showed 92.8% sensitivity and 75.0% specificity. ILD, GGO, and reticulation extents were 14.8%, 7.7%, and 7.1% on CT sQA and 13.0%, 11.2%, and 1.6% on CT QA. HC was <1% and not further considered. UTE intra-/inter-reader CCC were 0.92 and 0.89 for ILD extent and 0.84 and 0.79 for GGO extent. UTE RET extent intra-/inter-reader CCC were 0.22 and 0.18. UTE ILD and GGO extents CCC against CT sQA and QA were $\geq$0.93 and $\geq$0.88, respectively. RET extent CCC were 0.35 and 0.22 against sQA and QA, respectively.

Conclusion: UTE Spiral VIBE-MRI sequence is reliable in assessing ILD and GGO extents in systemic sclerosis-interstitial lung disease patients.

Key Words: magnetic resonance imaging, interstitial lung diseases, systemic sclerosis, x-ray computed tomography

(*J Thorac Imaging* 2022;00:000–000)

Systemic sclerosis (SSc) is an autoimmune disease characterized by fibrosis of the skin and internal organs, vasculopathy and immune dysregulation.[1] Moreover, interstitial lung disease (ILD) is a frequent complication and a major cause of death.[2] In SSc, different patterns of ILD may be encountered, such as nonspecific interstitial pneumonia and usual interstitial pneumonia.[3] About two-thirds of SSc patients show a nonspecific interstitial pneumonia pattern, usually characterized by ground-glass opacities (GGO) and reticulations (RET) on computed tomography (CT). The remaining third of SSc patients often display a usual interstitial pneumonia pattern, where the hallmark feature is represented by honeycombing (HC).[4–9] CT is the gold standard imaging technique[10,11] to assess SSc-related ILD (SSc-ILD). However, SSc patients may be younger than other ILD patients, with a peak of onset between 30 and 50 years.[12] Therefore, a radiation-free technique, such as magnetic resonance imaging (MRI), has been recently proposed for patients with ILD[13,14] and deserves to be taken into consideration. MRI of the pulmonary parenchyma is problematic to obtain because of the extremely low proton density of the lung tissue,[15] magnetic susceptibility of sharp air/parenchyma interfaces[16] and respiratory motion artifacts.[15] New MRI sequences, such as ultrashort echo-Time (UTE), have been designed to overcome these limitations, counteracting lung parenchyma T2 star-related signal decay.[15] Moreover, UTE allows isotropic voxels and multiplanar reconstructions acquiring data during free breathing conditions with fully automatic respiratory synchronization.[17]

This prospective study aimed to evaluate the reliability of an UTE-MRI sequence, denominated Spiral VIBE, in identifying SSc-ILD and quantifying the extents of SSc-ILD-related abnormalities, using CT as the reference standard.

From the *Department of Radiology, Ca' Foncello General Hospital, Treviso; †Department of Experimental and Clinical Biomedical Sciences, University of Florence & Radiodiagnostic Unit n. 2 AOUC; ‡Department of Experimental and Clinical Medicine, University of Florence and Division of Rheumatology AOUC & Scleroderma Unit; #Department of Experimental and Clinical Medicine, University of Florence & Division of Internal Medicine Unit IV AOUC, Florence, Italy; §Department of Pediatric Pulmonology, Erasmus University Medical Centre, Sophia Children's Hospital; ‖Department of Radiology, Erasmus University Medical Centre, Rotterdam, The Netherlands; and ¶MR Applications Predevelopment, Siemens Healthcare GmbH, Erlangen, Germany.

The authors declare no conflicts of interest.

Correspondence to: Nicholas Landini, MD, Department of Radiology, Ca' Foncello General Hospital, Piazzale dell'Ospedale, Treviso 31100, Italy (e-mail: nikolandini@hotmail.it).

DOI: 10.1097/RTI.0000000000000637

MATERIALS AND METHODS

Study Design

This was a prospective observational multicentric study (Department of Radiology, AOU Careggi, Florence, Italy and Department of Radiology, Ca' Foncello General Hospital, Treviso, Italy). From February 2019 to February 2020, consecutive SSc patients referred to the rheumatologic department (AOU Careggi, Florence, Italy), with suspected or ascertained ILD and in clinical need for a chest CT, were evaluated to undergo both chest CT and MRI examinations on the same day. SSc diagnosis was performed according to the 2013 ACR/EULAR criteria.[18] The exclusion criteria were: age below 18 years, heart failure or pulmonary disease other than ILD, contraindication to MRI, no informed consent, claustrophobia, impossibility to lay supine for the scan time and/or to follow breathing instructions, low-quality images for visual assessment or wrong software segmentation (see the paragraph on *Image analysis*). Patients were referred to one of the two radiologic centers based on geographical proximity and were instructed on how to perform the breathing maneuvers. Recorded data included: age, sex, antibody subset, previous and ongoing therapy, pulmonary function tests (ie, forced volume capacity and diffusion lung capacity for carbon monoxide) and presence of pulmonary arterial hypertension. The research project was approved by the local institutional ethics committees: CEAV Careggi, Florence, protocol number 27299/2019, code 15220/oss and CESC Treviso and Belluno, protocol number 641/CECEAV.

Imaging Systems and Acquisition Protocol

Chest CT scans were performed as follows: tube voltage 120 kV, tube current 200 mAs, slice thickness 1 mm, reconstruction kernels b35f and b60f and matrix 512×512. The CT scanners were a Sensation 64 and a Somatom Definition Flash (Siemens, Forchheim, Germany). Each CT acquisition took 3 to 5 seconds and was obtained at the end of full inspiration, without contrast agent administration.

UTE-MRI scans were performed with two 1.5 T MRI systems (Aera and Avanto Fit; Siemens, Erlangen, Germany). The 2 MRI systems supported the same UTE sequence and the same parameters: repetition time 3.73 ms, echo time 0.05 ms, flip angle 5 degrees, distance factor 20%, field of view 480×480, matrix 320×320, and voxel size 1.5×1.5×1.5 mm. UTE scans were free-breathing coronal acquisitions with a fully automated navigator trigger (Siemens-Dense). UTE scans lasted from 7 to 9 minutes, depending on the respiratory rhythm of the patients. No contrast agent was administrated. Images were reformatted in axial sections. All examinations were acquired with patients in supine position. Prone acquisitions, that might be performed to avoid the dependent atelectasis,[19] were considered uncomfortable and inefficiently performable in a great percentage of our patients, given the MRI examination duration and patients clinical conditions.

Image Analysis

CT and UTE scan quality was assessed in consensus by two chest radiologists of 10 and 12 years of experience in lung MRI (P.C. and G.M.). Scans were discarded as low-quality images in presence of significant blurring of airways and/or of peripheral lung parenchyma, as previously reported.[20] Then, two thoracic radiologists, each with 10 years of experience in thoracic imaging (N.L. and Me.O.), evaluated CT and UTE scans. First, they visually assessed the presence of ILD by the analysis of the whole parenchyma on both acquisitions. Then, they performed a visual semiquantitative analysis (sQA) on both CT and UTE to compute the disease extent of lung ILD-related abnormalities: GGO, RET and HC extents were scored as

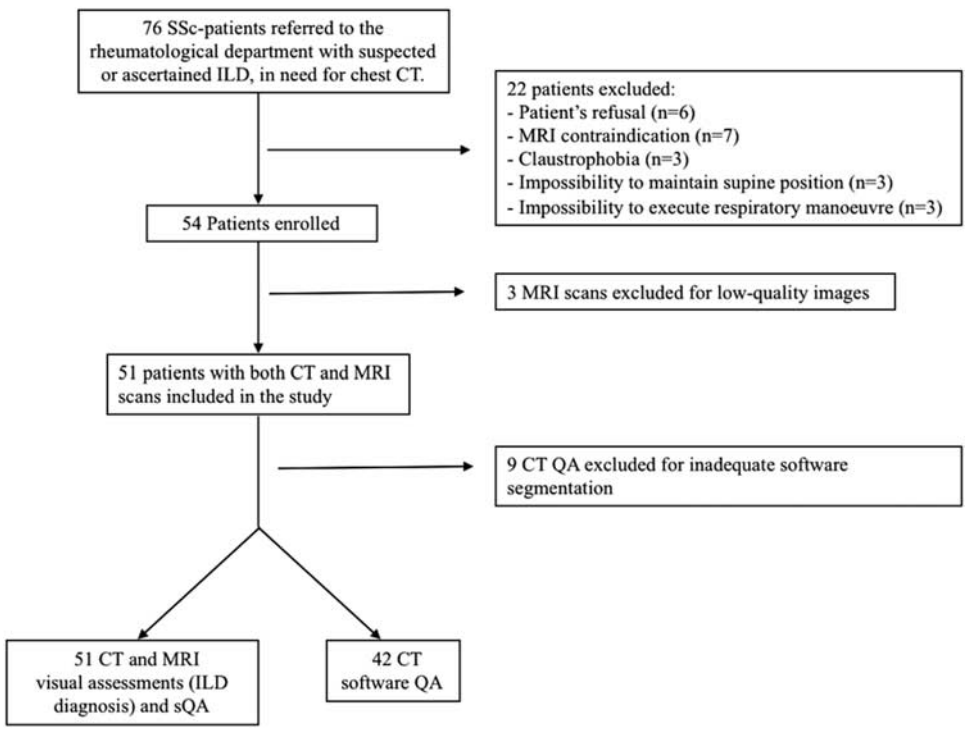

FIGURE 1. Detailed flowchart of patients' inclusion.

TABLE 1. Clinical, Functional, and Radiologic Characteristics of the SSc Population

Clinic and Radiology	CT sQA (n = 51)	UTE sQA (n = 51)	*P*	CT QA (n = 42)	UTE sQA (n = 42)	*P*
Age median (IQR)	50 (45-59)		—	49 (43-57)		—
Female (%)	43 (84)		—	38 (90)		—
SCL (%)	25 (61), n = 41		—	22 (59), n = 37		—
CENP-B (%)	13 (32), n = 41		—	13 (35)), n = 37		—
FVC median (IQR)	92 (70-109)		—	91 (70-104)		—
DLCO median (IQR)	59 (41-69)		—	57 (40-68)		—
IS therapy (%)	26 (62), n = 42		—	23 (62), n = 37		—
Steroid therapy (%)	19 (45), n = 42		—	18 (58), n = 31		—
Radiology						
ILD-Extent mean % (SD)	14.8 (22.8)	12.9 (19.2)	> 0.05	13.0 (19.7)	12.8 (19.9)	> 0.05
GGO % (SD)	7.7 (15.2)	9.8 (17.4)	> 0.05	11.2 (18.6)	9.7 (17.7)	> 0.05
RET % (SD)	7.1 (10.0)	3.0 (4.6)	0.012	1.6 (1.8)	3.1 (4.6)	0.049
HC % (SD)	0.0 (0.2)	0	NA	0.1 (0.3)	0	NA

CENP-B indicates anti-centromere B antibodies; DLCO, diffusion lung capacity for carbon monoxide; FVC, forced vital capacity; IQR, interquartile range; IS, immunosuppressive; n, patients' number; SCL, anti-topoisomerase 1 antibodies.

the percentage of involved lung parenchyma (at the nearest 5%) at 5 anatomic levels[21,22]: (1) aortic arch, (2) carina, (3) confluence of pulmonary veins, (4) halfway between levels 3 and 5, (5) immediately above the right hemidiaphragm. The ILD extent at each level was obtained summing the percentages of all abnormalities at that level. Then, the total GGO, RET, HC, and ILD extents were computed as the mean percentage of the 5 levels. For instance, if the GGO extent is 0%, 5%, 10%, 15%, and 20% for each of the five levels, the mean GGO extent was computed as (0+5+10+15 +20)/5 = 10% total lung parenchyma. Lung abnormalities were defined according to the radiological glossary of terms compiled by the Fleischner Society.[23] GGO was defined as hazy increased opacity, with preservation of bronchial and vascular margins. RET was defined as a collection of innumerable small linear opacities that, by summation, produce an appearance resembling a net. HC was defined as clustered cystic air spaces that are usually subpleural, peripheral, and basal in distribution; the walls of the cysts are well defined and often thick (1 to 3 mm).

CT images were analyzed with high-resolution kernel, b60f, using a standard lung window. UTE window was visually adjusted to obtain the best contrast-to-noise ratio. CT and UTE scans were analyzed separately. Readers assessed images independently and, after 1 month, 1 reader (N.L.) repeated the analysis. Lastly, both readers evaluated the images in consensus after an interval of 3 months. Discordances were discussed with a third senior radiologist (S.C.) with 30 years of experience in MRI imaging. In addition, an automated quantitative analysis (QA) of CT images was obtained on standard reconstruction algorithms (b35f) by using Imbio's Lung Texture Analysis software (Imbio LLC, Minneapolis, MN), based on Computer-Aided Lung Informatics for Pathology Evaluation and Rating (CALIPER) algorithm, as previously performed in SSc-ILD.[21] The software segments the lung into 3 areas (upper, middle, and lower), then identifies and quantifies percentages of GGO, RET and HC. The total ILD score is computed as the sum of all abnormalities. One thoracic radiologist (Me.O.) checked the software segmentations, ascertaining the inclusion of the whole lung parenchyma and the exclusion of other structures (ie, trachea).

TABLE 2. Intra-reader and Inter-reader Agreement in Semiquantitative Extent Analysis of total ILD and ILD-related Abnormalities, Expressed by Lin's Concordance Correlation Coefficients (95% Confidence Interval)

	CT sQA	UTE sQA
Intra-reader agreement		
ILD	0.95 (0.94-0.96)	0.92 (0.89-0.95)
GGO	0.96 (0.95-0.97)	0.84 (0.81-0.87)
RET	0.75 (0.75-0.77)	0.22 (0.18-0.25)
Inter-reader agreement		
ILD	0.94 (0.94-0.94)	0.89 (0.89-0.90)
GGO	0.92 (0.92-0.93)	0.79 (0.78-0.80)
RET	0.76 (0.75-0.78)	0.18 (0.16-0.20)

Statistical Analysis

Cohen κ test was used to compute intra-/inter-reader agreement for SSc-ILD diagnosis on CT and UTE. κ values of 0.01 to 0.20, 0.21 to 0.40, 0.41 to 0.60, 0.61 to 0.80, 0.81 to 0.99, and 1 represented poor, fair, moderate, substantial, almost perfect, and perfect agreement, respectively.[24] Sensitivity, specificity, positive and negative predictive values[25] of UTE were computed. Lin's concordance correlation coefficient (CCC)[26] was used to compute intra-/inter-reader agreement for SSc-ILD extent analyses and to compare UTE consensus reading for disease extent analysis with CT, namely UTE sQA versus CT sQA and QA. The CCC values of 0.00 to 0.10, 0.11 to 0.40, 0.41 to 0.60, 0.61 to 0.80, and 0.81 to 1.0 represented no, slight, fair, good, and very good agreement, respectively. Collected data were analyzed using the SPSS v. 23.0 statistical analysis software (IBM Corp., New York, NY; formerly SPSS Inc., Chicago, IL).

RESULTS

Patient Cohorts

Seventy-six patients were initially screened by a rheumatologist (M.O.) for CT and MRI examinations. Of these, 22 patients were excluded because of patient's refusal (n = 6), MRI contraindication (n = 7), claustrophobia (n = 3), difficulty to perform respiratory maneuvers (n = 3), and difficulty to maintain supine position (n = 3). Therefore, 54 patients performed both CT and MRI scans on the same day. All 54 CT scans were considered adequate in terms of image quality. Three UTE acquisitions (5.5%) were discarded because of blurring of peripheral lung parenchyma (2 UTE acquired on Aera, 1 on Avanto Fit). Thus, 51 patients (94.5%) were included in the study (33 UTE scanned with Aera, 18 with Avanto Fit). Furthermore, of them,

TABLE 3. Lin's Concordance Correlation Coefficient Between CT and UTE for ILD, GGO, and RET Extents (95% Confidence Interval)

	CT sQA vs. UTE sQA	CT QA vs. UTE sQA
ILD	0.95 (0.94-0.95)	0.89 (0.88-0.90)
GGO	0.93 (0.93-0.94)	0.88 (0.87-0.88)
RET	0.35 (0.34-0.36)	0.22 (0.21-0.23)

9 CT QA were discarded because of wrong segmentations; thus, 42 patients were considered to compare UTE with CT QA. The detailed flowchart of patients' inclusion is shown in Figure 1. Demographical, serological, and clinical characteristics of the patients are reported in Table 1.

ILD Presence and Extent

SSc-ILD was detected in 76.5% (39/51) on both CT and UTE sequences. The percentage of lung parenchyma affected by ILD, calculated as the mean value of all patients, was 14.8% and 12.9% on CT sQA and UTE sQA, respectively. The mean ILD extents of the 42 patients with available CT QA were 13.0% on CT QA and 12.8% on UTE sQA. All alterations extents are shown in Table 1. HC extent was found to be lower than 1% in all extent assessments and therefore considered irrelevant for further analysis.

Observers Agreements

Intra-reader Cohen κ for ILD diagnosis showed almost perfect agreement for CT ($\kappa = 0.95$) and moderate agreement for UTE ($\kappa = 0.56$).

Intra-reader agreement for extent analyses was good to very good for total ILD, GGO, and RET on CT sQA (CCC ranging from 0.75 to 0.96). UTE sQA showed good to very good intra-reader agreement for ILD extent (CCC = 0.92) and GGO extent (CCC = 0.84), but poor for RET extent (CCC = 0.22) (Table 2). Inter-reader Cohen κ for ILD diagnosis showed substantial agreement ($\kappa = 0.74$) for CT and fair agreement for UTE ($\kappa = 0.26$). Inter-reader agreements for alterations extents were good to very good (CCC ranging from 0.76 to 0.94) for total SSc-ILD, GGO, and RET on CT sQA. UTE sQA showed very good inter-reader agreement for the ILD extent (CCC = 0.89) and good agreement for the GGO extent (CCC = 0.79), but poor inter-reader agreement for RET (CCC = 0.18) (Table 2).

UTE-MRI Performance

UTE sensitivity, specificity, and positive and negative predictive values (confidence interval) in identifying SSc-ILD on consensus reading were 92.3% (79.1% to 98.4%), 75.0% (42.8% to 94.5%), 92.3% (79.1% to 98.4%), and 75.0% (42.8% to 94.5%), respectively. In particular, UTE generated 3 false negatives (ILD extent on CT sQA 1%, 3%, and 3%) and 3 false positives (ILD extent on UTE 5%, 6% and 8%). The alterations extent CCC between UTE and CT (sQA and QA) were very good for total ILD (0.95 and 0.89) and GGO extent (0.93 and 0.88), whereas poor for the RET extent (0.35 and 0.22) (Table 3).

DISCUSSION

We tested the performance of UTE Spiral VIBE in the detection of SSc-ILD and in the assessment of disease extent, using CT as the reference standard. UTE Spiral VIBE proved to be reliable in ILD and GGO extent analysis (Figs. 2, 3). Thus, in our series the potential benefits deriving from new chest MRI techniques, as reported in state-of-art reviews,[14,27] are confirmed.

The first paper that investigated the use of MRI in ILD extent assessment on SSc patients[28] used a 2D BH half-Fourier single-shot TSE sequence. This 2D sequence showed high sensitivity to detect SSc-ILD, but it was less reliable in evaluating the disease extent. Generally, UTE sequences help overcome the technical limits of MRI in the lung study by enabling both high signal-to-noise ratio and high-resolution 3D lung morphological imaging. In fact, UTE sequences reduce the minimum time needed to cover k-space using a nonselective RF pulse. In particular, standard Cartesian phase encoding and spiral sampling in-plane encoding are performed in the UTE Spiral VIBE tested by us.[17] Previous studies have found good agreement of UTE sequences with CT in ILD detection,[17,29] but none of these assessed the ability to quantify disease extent. The current study is the first one, as far as we know, that demonstrated the agreement between a UTE sequence and CT in SSc-ILD extent evaluation.

Moreover, UTE Spiral VIBE acquisitions did not exceed the 8-minute duration in our study and only 5% of them (3/54) were discarded for motion artifacts. This was a relevant result, as a short scan time is pivotal in dyspneic patients, such as those

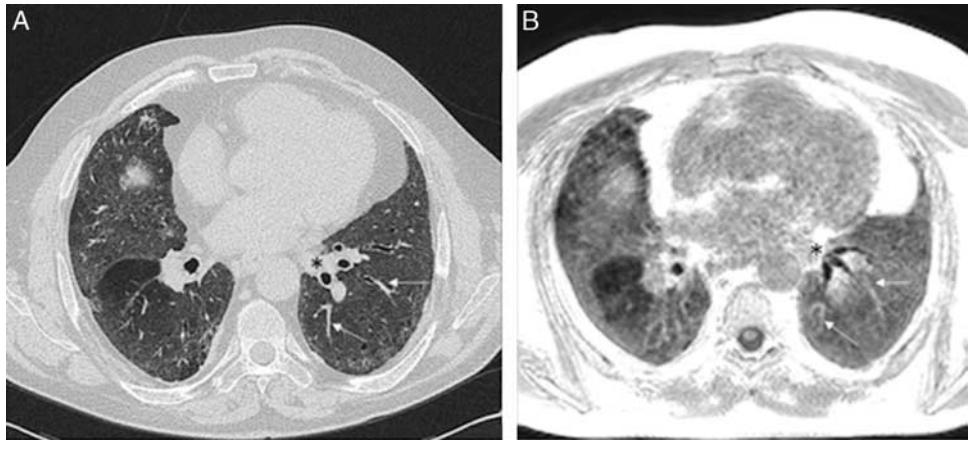

FIGURE 2. CT and UTE sQA SSc-ILD extent analysis. ILD was scored as 85% total lung parenchyma at level 5 on both CT (A) and UTE (B). Breath-hold CT and free-breathing UTE acquisitions may lead to slightly anatomical differences at the same level, as it was shown by left lower lobe bronchi (black asterisks); however, visualized segmental vessels are the same (white arrows).

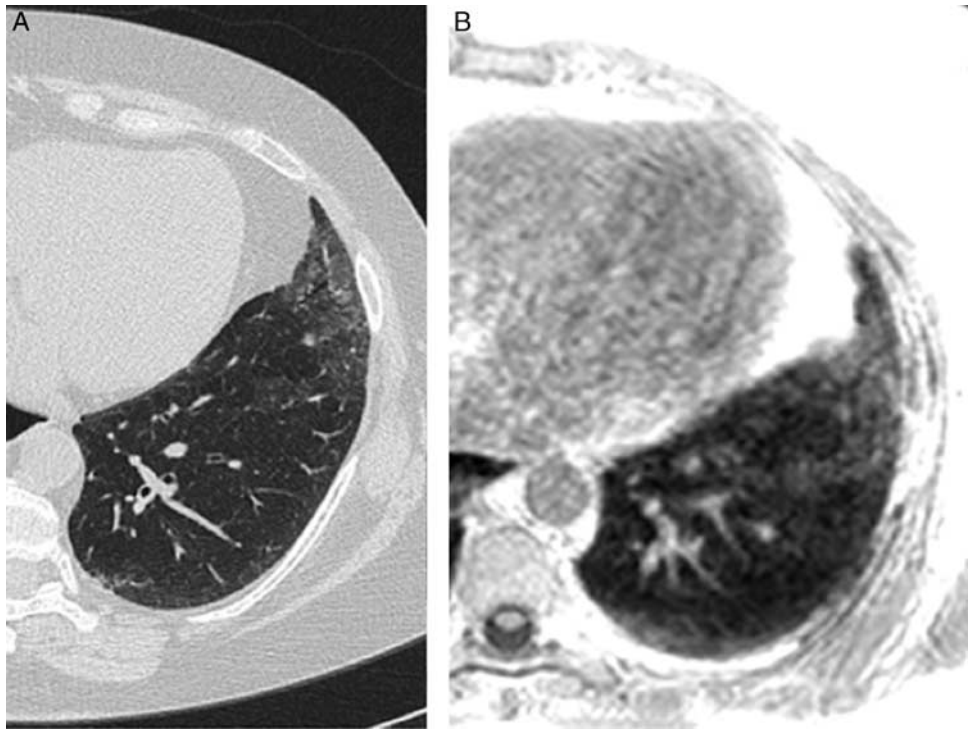

FIGURE 3. SSc-ILD, left lung: ground-glass opacities on CT and UTE. CT areas of ground-glass opacities (A) may be easily recognized and quantified on UTE (B).

with SSc-ILD.[3] Our Spiral VIBE exploits an improved automated respiratory gating that should make the scan more robust against motion artifacts than a previous zero-TE version, namely PETRA (Pointwise-Encoding-Time-Reduction-Radial-Acquisition). In fact, PETRA relies on navigator positioning with possible steady-state interruption and longer acquisition time, depending on the required resolution and actual breathing pattern of patients.[17]

We also observed high sensibility and positive predictive value of UTE in ILD diagnosis, but intra-/inter-reader

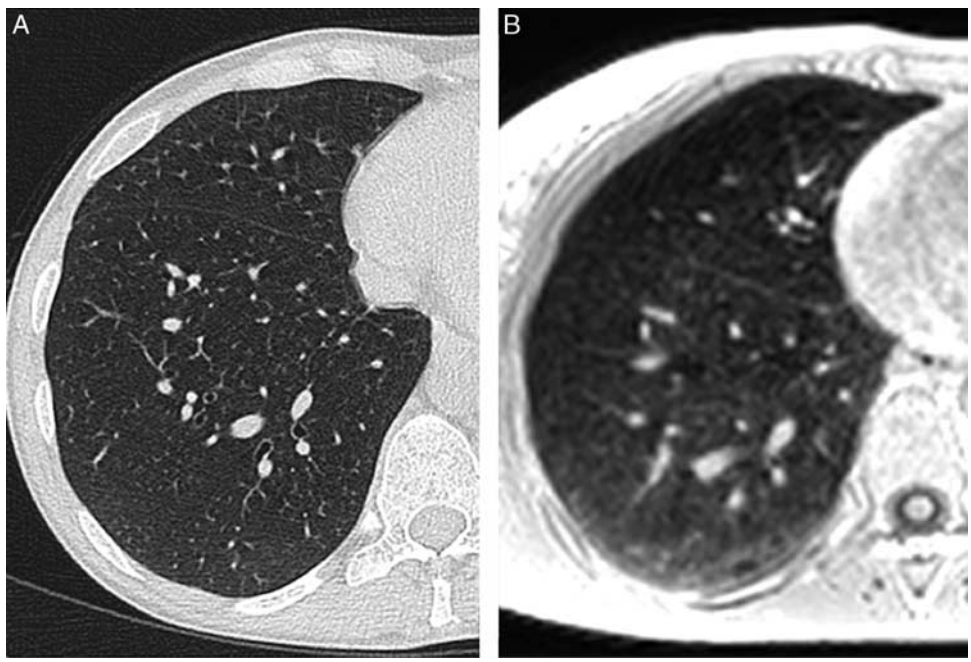

FIGURE 4. SSc-ILD, right lung: possible cause of disagreement in ILD detection on UTE. If ILD is absent or mild on CT (A), ground-glass opacities on UTE (B) could be entirely interpreted as dependent atelectasis or ILD.

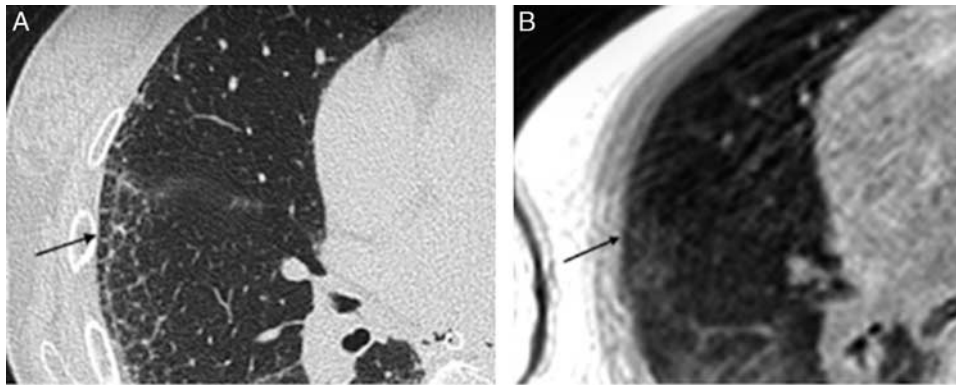

FIGURE 5. SSc-ILD, particular of the right lung: reticulations assessment. Compared with CT (A), reticulations may be misinterpreted in UTE (B), partially resembling ground-glass opacities (black arrows).

agreements were lower than CT, for such task. As a matter of fact, especially in mild or no ILD, the assessment of lung parenchyma in expiration could have artificially increased the detection of GGO. The lung parenchyma in expiration has higher signal for partial collapse (atelectasis), especially in the dependent peripheral lung regions, that may be also the zones primarily affected by SSc-ILD.[8] This could justify the readers' discrepancy, since the dependent GGO due to mild interstitial disease may be misinterpreted as partial alveolar collapse (atelectasis) and *vice versa*, as well as it may lies behind the UTE false negatives and false positives (Fig. 4). To overcome this problem, UTE could be acquired at full inspiration, as recently shown by Veldhoen et al.[30] They achieved the best spatial and temporal resolution compromise with a breath-hold UTE of 2.3 mm (isotropic voxel) for a mean scan time of 115 seconds obtained with 5 breath-holds, to cover the entire thorax. However, the setting proposed by Veldhoen et al[30] requires a significant effort to the patient providing anyhow a spatial resolution lower than CT, since inspiration and the small voxel size could reduce lung signal, affecting ILD evaluation. Nevertheless, considering the good performance in quantifying ILD and GGO extent, UTE could be now tested to monitor disease progression, especially in young patients with ascertained ILD and GGO as the predominant feature. In the clinical setting, a good policy to improve UTE diagnostic accuracy could be to acquire a baseline MRI scan at the same time of CT. Then, in selected subjects, MRI could be alternated to CT, adapting an imaging scheme adopted for other chronic lung diseases, such as cystic fibrosis.[31] However, further studies are needed to confirm this hypothesis.

Nevertheless, RET analysis in UTE sequence was scarcely reliable. Air-filled alveoli tend to reduce the lung signal[15] and might make the identification of thickened septa very challenging. Moreover, adjacent or superimposed areas GGO, due to ILD or partial alveolar collapse, could partially hide septal thickening (Fig. 5). Thus, the assessment of fine RET extent remains a limitation of chest MRI, even with UTE sequences.

Strengths of our study included the non-small number of patients and the same-day acquisition of CT and MRI, as well as the CT QA analysis. However, we have to acknowledge some limitations. First, anatomical levels for sQA could have slightly differed between full inspiration on CT and free breathing scans on UTE. However, sQA performed in the current study is a well-validated sampling method for a diffuse lung disease, such as SSc-ILD, that should be representative of the whole lung parenchyma[32] and small differences in anatomical levels (Fig. 2) should not be so relevant in quantifying the disease. Moreover, we tested UTE also against CT QA, that is a whole lung parenchyma evaluation, and we obtained similar correlation results. To avoid the possible level mismatch in sQA, one solution could have been a whole-lung visual evaluation for both CT and UTE. However, among visual ILD scoring systems that are usually considered for SSc, if the whole parenchyma is evaluated by the analysis of each lobe, the total score is based on wider ranges of involvement percentage (ie, assigning one point for each 25%, per each lobe)[32]: this scoring system, in our opinion, may result in a more approximated quantification. On the other hand, assessing the whole lobes to the nearest 5% of involvement would be really challenging and scarcely feasible in a clinical setting. Second, the low extent of HC on CT images made difficult to assess the full diagnostic potential of UTE for this kind of alterations being HC less common than GGO combined with RET in SSc-ILD.[3] Then, we could not compare the image quality of the UTE sequence obtained with the two different MRI systems, which would have required scanning twice the same patient in both systems. For further multicenter studies, protocol harmonization will be needed to reduce image quality variability. Lastly, we did not correlate imaging data to clinical and lung function status, but this was beyond the purpose of our work.

In conclusion, the respiratory-triggered Spiral VIBE MRI sequence is a reliable imaging tool in ILD and GGO extent analysis in SSc-ILD patients, although it may suffer from low inter-reader agreement in mild ILD diagnosis. However, RET extent assessment remains challenging for this MRI sequence.

REFERENCES

1. Orlandi M, Lepri G, Damiani A, et al. One year in review 2020: systemic sclerosis. *Clin Exp Rheumatol*. 2020;38(suppl 125): 3–17.
2. Volkmann ER, Fischer A. Update on morbidity and mortality in systemic sclerosis–related interstitial lung disease. *J Scleroderma Relat Disord*. 2021;6:11–20.
3. Perelas A, Silver RM, Arrossi AV, et al. Systemic sclerosis-associated interstitial lung disease. *Lancet Respir Med*. 2020;8: 304–320.
4. Desai SR, Veeraraghavan S, Hansell DM, et al. CT features of lung disease in patients with systemic sclerosis: comparison with

idiopathic pulmonary fibrosis and nonspecific interstitial pneumonia. *Radiology*. 2004;232:560–567.
5. Fujita J. Non-specific interstitial pneumonia as pulmonary involvement of systemic sclerosis. *Ann Rheum Dis*. 2001;60:281–283.
6. Goldin JG, Lynch DA, Strollo DC, et al. High-resolution CT scan findings in patients with symptomatic scleroderma-related interstitial lung disease. *Chest*. 2008;134:358–367.
7. King TE. Nonspecific interstitial pneumonia and systemic sclerosis. *Am J Respir Crit Care Med*. 2002;165:1578–1579.
8. Launay D, Remy-Jardin M, Michon-Pasturel U, et al. High resolution computed tomography in fibrosing alveolitis associated with systemic sclerosis. *J Rheumatol*. 2006;33:1789–1801.
9. Suliman S, Al Harash A, Roberts WN, et al. Scleroderma-related interstitial lung disease. *Respir Med Case Rep*. 2017;22:109–112.
10. Solomon JJ, Olson AL, Fischer A, et al. Scleroderma lung disease. *Eur Respir Rev*. 2013;22:6–19.
11. Picano E, Semelka R, Ravenel J, et al. Rheumatological diseases and cancer: the hidden variable of radiation exposure. *Ann Rheum Dis*. 2014;73:2065–2068.
12. Alba MA, Velasco C, Simeón CP, et al. Early- versus late-onset systemic sclerosis: differences in clinical presentation and outcome in 1037 patients. *Medicine (Baltimore)*. 2014;93:73–81.
13. Qian Y, Boada FE. Acquisition-weighted stack of spirals for fast high-resolution three-dimensional ultra-short echo time MR imaging. *Magn Reson Med*. 2008;60:135–145.
14. Romei C, Turturici L, Tavanti L, et al. The use of chest magnetic resonance imaging in interstitial lung disease: a systematic review. *Eur Respir Rev*. 2018;27:180062.
15. Miller GW, Mugler JP, Sá RC, et al. Advances in functional and structural imaging of the human lung using proton MRI. *NMR Biomed*. 2014;27:1542–1556.
16. Wild JM, Marshall H, Bock M, et al. MRI of the lung (1/3): methods. *Insights Imaging*. 2012;3:345–353.
17. Dournes G, Yazbek J, Benhassen W, et al. 3D ultrashort echo time MRI of the lung using stack-of-spirals and spherical k-Space coverages: evaluation in healthy volunteers and parenchymal diseases. *J Magn Reson Imaging*. 2018;48:1489–1497.
18. van den Hoogen F, Khanna D, Fransen J, et al. 2013 classification criteria for systemic sclerosis: an American college of rheumatology/European league against rheumatism collaborative initiative. *Ann Rheum Dis*. 2013;72:1747–1755.
19. Sundaram B, Chughtai AR, Kazerooni EA. Multidetector high-resolution computed tomography of the lungs: protocols and applications. *J Thorac Imaging*. 2010;25:125–141.
20. Bae K, Jeon KN, Hwang MJ, et al. Comparison of lung imaging using three-dimensional ultrashort echo time and zero echo time sequences: preliminary study. *Eur Radiol*. 2019;29:2253–2262.
21. Occhipinti M, Bosello S, Sisti LG, et al. Quantitative and semi-quantitative computed tomography analysis of interstitial lung disease associated with systemic sclerosis: a longitudinal evaluation of pulmonary parenchyma and vessels. *PLoS One*. 2019;14:e0213444.
22. Hansell DM, Bankier AA, MacMahon H, et al. Fleischner Society: glossary of terms for thoracic imaging. *Radiology*. 2008;246:697–722.
23. Goh NS, Desai SR, Veeraraghavan S, et al. Interstitial lung disease in systemic sclerosis: a simple staging system. *Am J Respir Crit Care Med*. 2008;177:1248–1254.
24. McHugh ML. Interrater reliability: the kappa statistic. *Biochem Med (Zagreb)*. 2012;22:276–282.
25. Parikh R, Mathai A, Parikh S, et al. Understanding and using sensitivity, specificity and predictive values. *Indian J Ophthalmol*. 2008;56:45–50.
26. Lin LI-K. A concordance correlation coefficient to evaluate reproducibility. *Biometrics*. 1989;45:255–268.
27. Weatherley ND, Eaden JA, Stewart NJ, et al. Experimental and quantitative imaging techniques in interstitial lung disease. *Thorax*. 2019;74:611–619.
28. Pinal-Fernandez I, Pineda-Sanchez V, Pallisa-Nuñez E, et al. Fast 1.5 T chest MRI for the assessment of interstitial lung disease extent secondary to systemic sclerosis. *Clin Rheumatol*. 2016;35:2339–2345.
29. Ohno Y, Koyama H, Yoshikawa T, et al. Pulmonary high-resolution ultrashort TE MR imaging: comparison with thin-section standard- and low-dose computed tomography for the assessment of pulmonary parenchyma diseases. *J Magn Reson Imaging*. 2016;43:512–532.
30. Veldhoen S, Heidenreich JF, Metz C, et al. Three-dimensional ultrashort echotime magnetic resonance imaging for combined morphologic and ventilation imaging in pediatric patients with pulmonary disease. *J Thorac Imaging*. 2021;36:43–51.
31. Kuo W, Ciet P, Tiddens HA, et al. Monitoring cystic fibrosis lung disease by computed tomography. Radiation risk in perspective. *Am J Respir Crit Care Med*. 2014;189:1328–1336.
32. Assayag D, Kaduri S, Hudson M, et al. High resolution computed tomography scoring systems for evaluating interstitial lung disease in systemic sclerosis patients. *Rheumatology*. 2012:S1–003.